Hindawi Publishing Corporation
Journal of Nanomaterials
Volume 2016, Article ID 7659074, 9 pages
http://dx.doi.org/10.1155/2016/7659074

Research Article

Induced Magnetic Anisotropy in Liquid Crystals Doped with Resonant Semiconductor Nanoparticles

Vicente Marzal, Juan Carlos Torres, Isabel Pérez, José Manuel Sánchez-Pena, and Braulio García-Cámara

Displays and Photonic Applications Group, Electronic Technology Department, Carlos III University of Madrid, Leganés, 28911 Madrid, Spain

Correspondence should be addressed to Braulio García-Cámara; brgarcia@ing.uc3m.es

Received 10 April 2016; Accepted 28 June 2016

Academic Editor: Nathan C. Lindquist

Currently, there are many efforts to improve the electrooptical properties of liquid crystals by means of doping them with different types of nanoparticles. In addition, liquid crystals may be used as active media to dynamically control other interesting phenomena, such as light scattering resonances. In this sense, mixtures of resonant nanoparticles hosted in a liquid crystal could be a potential metamaterial with interesting properties. In this work, the artificial magnetism induced in a mixture of semiconductor nanoparticles surrounded by a liquid crystal is analyzed. Effective magnetic permeability of mixtures has been obtained using the Maxwell-Garnett effective medium theory. Furthermore, permeability variations with nanoparticles size and their concentration in the liquid crystal, as well as the magnetic anisotropy, have been studied.

1. Introduction

Plasmonics is a consolidated research field, due to its potential applications in many nanotechnology domains [1–3]. Plasmon resonances occur when the photon frequency of an incident radiation is resonant with the collective oscillation of the conduction electrons in a metal. This process involves the concentration of light in subwavelength dimensions which allows the manipulation of light at nanoscale. This phenomenon is the basis of a myriad of applications, ranging from new all-optical devices [4, 5] to the design of metatoms to perform metamaterials with tunable optical properties [6–8].

Although huge efforts have been made on plasmon nanoparticles and plasmonic applications [9], metallic samples have the inherent problem of absorption in the visible range. This absorption produces thermal effects leading to material degradation. Semiconductor materials with high refractive index can be the alternative to plasmonic materials (e.g., gold and silver) in this kind of applications. The magnetic and electric Mie resonances in light scattering of semiconductor materials [10, 11] are analogous to the localized surface plasmon resonances in metallic nanoparticles. These semiconductor nanoparticles can act as photonic nanoresonators due to the high-refractive-index contrast between them and the surrounding medium and the ratio between their size and the incident radiation wavelength. These properties lead to the appearance of both magnetic and electric resonances in the visible range of the electromagnetic spectrum [12]. The excitation of these resonances is being deeply studied nowadays. For instance, astonishing phenomena, like scattering directionality, have been reported [13, 14] in these systems. In addition, the low optical absorption of semiconductors has overcome in part thermal issues [15].

The tunability of resonances of these nanostructures is a key aspect for several applications. For instance, the spectral coincidence of these resonances with the absorption peak of different molecules is the basis of chemical sensors [16]. As in plasmonics, Mie resonances of dielectric nanoparticles can be tuned changing their size, shape, composition, or the optical properties of the surrounding medium. The variation of the properties of the nanoparticles is a static method: it involves the fabrication of new ones in order to change the output response, limiting its application. Nevertheless, the change of the surrounding medium properties may be dynamic. By using an active material as surrounding medium, its

optical properties can be changed with real time control and reversibility capacity, changing the resonant wavelength in the same way. This dynamic response is very interesting for applications such as active polarizers [17] or new tools for active photonic circuits [18].

Among all the active media used in plasmonic devices, liquid crystals are a good choice: they have capacity to easily modify their refractive index by electrical [19], optical [20], or thermal techniques [21] because of their high birefringence and small elastic constants. This control feature besides their high compatibility with optoelectronic materials makes them the perfect option as active dielectric media. Liquid crystal properties have also led to the development of a large variety of photonic devices (modulators, filters, optical switches, and so on) [22–24].

While liquid crystals have a remarkable dielectric anisotropy, their magnetic properties in the visible range do not have a noticeable behavior. In this sense, this work is devoted to analyze the magnetic properties of mixtures composed of a liquid crystal doped with semiconductor nanoparticles with magnetic resonances. The magnetic permeability of the nanoparticles and the effective magnetic permeability of the mixture have been studied in a set of simulations. The Maxwell-Garnett effective medium approach has been considered in the calculus of the permeability [25]. Searching a noticeable magnetic anisotropy, several liquid crystals and semiconductor nanoparticles have been considered.

2. Theory

The effective permeability, μ_{eff}, of mixtures composed of a liquid crystal (LC) doped with resonant nanoparticles (NPs) can be obtained through several effective medium approximations. In particular, a generalization of the Maxwell-Garnett Theory (MG) [25] has been considered in this work. This theory establishes that the effective dielectric function, ϵ_{eff}, of a matrix with homogeneous spherical inclusions can be expressed in terms of the optical properties of each component and the volume fraction of the inclusions (f) [26] as follows:

$$\epsilon_{\text{eff}} = \epsilon_m \left[1 + \frac{3f\left(\left(\epsilon - \epsilon_m\right)/\left(\epsilon + 2\epsilon_m\right)\right)}{1 - f\left(\left(\epsilon - \epsilon_m\right)/\left(\epsilon + 2\epsilon_m\right)\right)} \right], \quad (1)$$

where ϵ and ϵ_m are the dielectric permittivity of the inclusions and the matrix material, respectively.

Due to the symmetric nature of the electromagnetic field, an analogue expression can be derived for the effective magnetic permeability, μ_{eff}:

$$\mu_{\text{eff}} = \mu_h \left[1 + \frac{3f\left(\left(\mu_s - \mu_h\right)/\left(\mu_s + 2\mu_h\right)\right)}{1 - f\left(\left(\mu_s - \mu_h\right)/\left(\mu_s + 2\mu_h\right)\right)} \right], \quad (2)$$

where μ_h and μ_s are the magnetic permeability of the host medium and the inclusion, respectively.

In this work, a LC host medium with high-refractive-index semiconductor nanoparticles as inclusions is considered. Selected NPs have both electric and magnetic resonances in the visible range, although they are composed of nonmagnetic materials (e.g., silicon and germanium) [11]. Thus, effective optical constants can also be derived for the individual nanoparticles. Focusing attention on the magnetic properties, the effective magnetic permeability of these nanoparticles has been obtained through the Mie theory [26].

The scattered electromagnetic field (E_s, H_s) of a spherical particle (of radius R) made of a certain material, embedded in a homogeneous and isotropic media, can be calculated through the Mie theory [26]. This theory considers an expansion of the scattered fields in vector spherical harmonics ($N_{e1n}, M_{o1n}, N_{o1n}, M_{e1n}$), when the sphere is radiated with an incident electromagnetic plane wave with wavelength λ and amplitude E_0 :

$$E_s = E_0 \sum_{n=1}^{\infty} i^n \frac{2n+1}{n(n+1)} \left(i a_n N_{e1n} - b_n M_{o1n} \right),$$
$$H_s = \frac{k}{\omega\mu} E_0 \sum_{n=1}^{\infty} i^n \frac{2n+1}{n(n+1)} \left(i b_n N_{o1n} + a_n M_{e1n} \right), \quad (3)$$

where k is the wave vector and ω is the frequency of the incident field, μ is the magnetic permeability of the surrounding medium, and a_n, b_n, are the so-called Mie coefficients for the scattered field. Applying the boundary conditions between the sphere and the surrounding medium, analytical expressions for these coefficients can be deduced [26]:

$$a_n = \frac{\widetilde{m}\Psi_n(mx)\Psi_n'(x) - \Psi_n(x)\Psi_n'(mx)}{\widetilde{m}\Psi_n(mx)\xi_n'(x) - \xi_n(x)\Psi_n'(mx)},$$
$$b_n = \frac{\Psi_n(mx)\Psi_n'(x) - \widetilde{m}\Psi_n(x)\Psi_n'(mx)}{\Psi_n(mx)\xi_n'(x) - \widetilde{m}\xi_n(x)\Psi_n'(mx)}. \quad (4)$$

Ψ_n and ξ_n are the Riccati-Bessel functions and $m = n_s/n$ is the relative refractive index between the sphere (n_s) and the surrounding medium (n). The factor $\widetilde{m}$ is given by $\widetilde{m} = m/\mu_s$, where μ_s is the magnetic permeability of the sphere material. The size parameter is x, which is given by the relation $x = 2\pi Rn/\lambda$, where R is the radius of the sphere and λ the incident wavelength, as was commented. While a_n coefficients are related to the electric response of the system, b_n are usually related to the magnetic character. In addition, a_1 and b_1 correspond to the dipolar behavior, a_2 and b_2 with the quadrupolar one, and so on.

These complex expressions can be simplified under certain assumptions, for instance, applying the Rayleigh approximation, which is satisfied when

$$x \ll 1,$$
$$|m|\, x \ll 1. \quad (5)$$

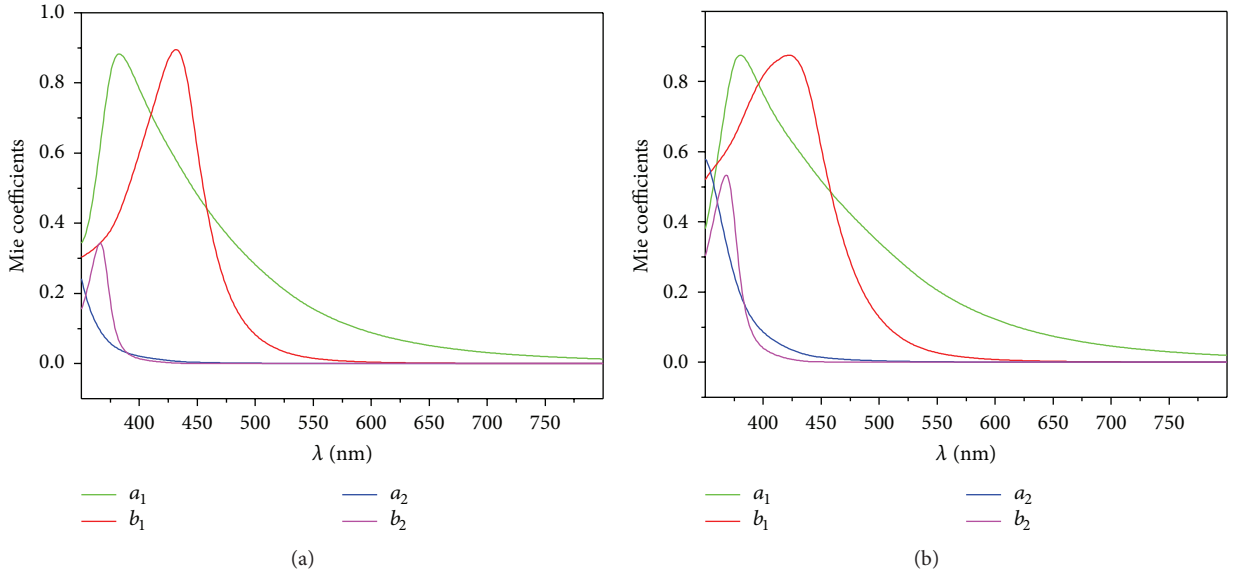

Figure 1: First four Mie coefficients of an AlAs nanoparticle, with a radius of 58 nm, embedded in liquid crystal (UCF-N3b) as a function of the incident wavelength.

In this case, only the dipolar components remain, and the expressions of Mie coefficients can be simplified as follows [26]:

$$a_1 = -i\frac{2x^3}{3}\frac{\epsilon - 1}{\epsilon + 2}, \tag{6}$$

$$b_1 = -i\frac{2x^3}{3}\frac{\mu - 1}{\mu + 2}, \tag{7}$$

$$a_n \approx b_n \approx 0; \quad n \geq 2. \tag{8}$$

This approximation is only satisfied by dipole-like spheres. Although the magnetic response of semiconductor nanoparticles has been observed in large nanoparticles (diameter > 50 nm), a simple analysis of the Mie coefficients shows that the dipolar character dominates in these nanoparticles in the visible wavelength range. Figure 1 shows the first four Mie coefficients (a_1, a_2, b_1, b_2) of an AlAs nanoparticle with a radius of $R = 58$ nm as a function of the incident wavelength, considering the ordinary refractive index (a) and the extraordinary refractive index (b) for the surrounding UCF-N3b LC host [27]. Although liquid crystals are not isotropic media, they can be approximated as isotropic considering either their ordinary or extraordinary refractive index. For the wavelength range where the magnetic resonance arises ($\lambda \approx$ 400 nm–450 nm), it can be seen that the dipolar contributions (a_1 and b_1) are dominant, allowing the assumption of a dipole-like sphere.

The effective magnetic permeability of these semiconductor nanoparticles has been obtained following the next procedure. Using homemade computer routines, the value of the Mie coefficient b_1 of the nanoparticle, considering it surrounded by the LC medium, has been calculated. Assuming that the spherical particle accomplishes the Rayleigh approximation, at least in a wavelength range, an effective value of the magnetic permeability, μ_s, of the particle has been deduced from expression (7). This value, along with the magnetic permeability of LC host, has been used to obtain the effective magnetic permeability of the mixture by means of the effective medium theory (see (2)). The refractive indices of liquid crystals have been obtained using the Cauchy model [27–32], and the optical properties of the NPs materials have been derived from references [33–37].

3. Process and Results

In order to obtain a maximum magnetic response, several liquid crystals, as well as semiconductor materials, have been considered. All materials have been selected based on the availability of data in the literature.

In this sense, analytical calculations considering 14 different liquid crystals as host (5PCH, E7, E44, MLC-6241-000, MLC-6608, MLC-9200-000, MLC-9200-100, TL-216, 5CB, BL038, DNDA-OC3, UCF-35, UCF-N3b, and W1825K) and 8 materials as doping NPs (AlAs, AlSb, GaAs, GaP, InGaAs, GaInP, Si, and TiO_2) have been carried out. In the following sections, only results related to those materials that maximize the effective magnetic permeability are shown.

3.1. Magnetic Resonances of Nanoparticles: Spectral Range. In this section, the optical behavior of an isolated nanoparticle embedded in a liquid crystal host is analyzed in order to check the appearance of a magnetic response and the spectral range in which it remains.

Considering each semiconductor material, listed above, the first four Mie coefficients (a_1, a_2, b_1, b_2) have been calculated. Nanoparticles radius has been selected in the range from 35 to 150 nm. Although these nanoparticle sizes do not strictly satisfy the Rayleigh criterion, we have obtained that the dipolar character is dominant in the spectral range of

Table 1: Summary of the most important parameters of the magnetic resonances of semiconductor nanoparticles embedded in liquid crystals. Only those cases presenting the most noticeable results have been included.

Mixture	Nanoparticle radius (nm)	Ordinary		Extraordinary	
		λ_0 (nm)	$\Delta\lambda$ (nm)	λ_0 (nm)	$\Delta\lambda$ (nm)
MLC6608 + AlAs	52	403	380–450	402	385–450
MLC6608 + AlSb	59	546	498–600	546	504–600
MLC6608 + GaAs	87	686	609–800	683	618–800
MLC6608 + GaInP	78	576	553–690	574	555–700
MLC6608 + GaP	50	464	430–500	463	437–510
MLC6608 + InGaAs	75	626	596–740	625	605–770
MLC6608 + Si	86	692	608–790	691	615–800
MLC6608 + TiO_2	77	496	487–640	492	490–650

the magnetic resonance. Nanoparticles have been considered embedded in the liquid crystal under its extreme optical conditions: the ordinary and the extraordinary refractive indices. In addition, although the calculations have been made for an isolated nanoparticle, the low concentration of NP in feasible experimental mixtures involves a low nanoparticle-nanoparticle interaction and their properties are close to those of the isolated case. This analysis has been made in a global spectral range between 350 nm and 800 nm. The attention has been placed on the analysis of the coefficient b_1, which is related to a magnetic dipolar behavior. All the selected materials have a remarkable b_1 contribution in an extended range of the visible spectrum. Table 1 summarizes the most important parameters derived from the simulations along with the LC host and NPs material. These parameters are the wavelength at which the magnetic resonance of the nanoparticle is centered, the spectral range where the dipolar term has predominance over the quadrupolar terms, and the nanoparticle radius which maximizes the magnetic resonance. These data have been obtained considering the ordinary and the extraordinary refractive indices of the liquid crystal. From Table 1, it can be seen that MLC6608 LC gives the most remarkable results. It will be seen in the next section that, despite the large list of LC analyzed, only two of them offer optimum results.

3.2. Effective Magnetic Permeability of NPs. Although nanoparticle materials are not magnetic in the visible range, in previous sections it has been seen that NPs have a prominent magnetic response at a certain spectral range. Under the assumption of the dominant-dipolar behavior, an effective magnetic permeability can be deduced for these nanoparticles. As it was explained above, this permeability can be derived from the magnetic dipole term (b_1), under the Rayleigh approximation (7).

In this work, it has been obtained that the magnetic response of semiconductor nanoparticles remains when they are embedded in a liquid crystal, presenting a nonunitary effective magnetic permeability at certain wavelengths range. As an example, Figure 2 shows the effective magnetic permeability of an AlSb nanoparticle of radius 58 nm embedded in a W1825K liquid crystal host, for both ordinary and extraordinary refractive indices of the LC. As it can be seen,

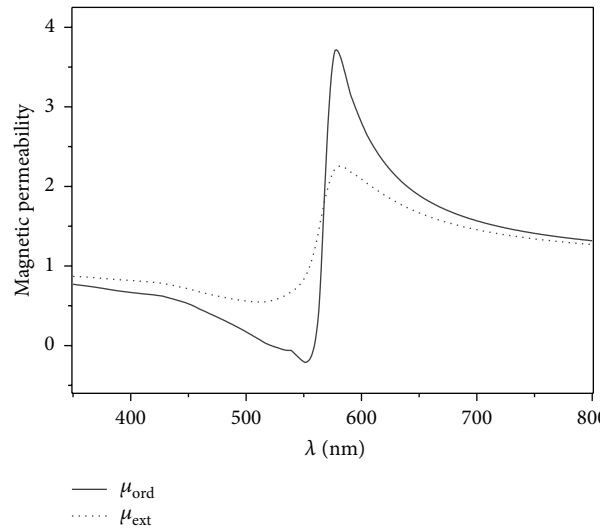

Figure 2: Magnetic permeability of an AlSb nanoparticle of 58 nm radius within the liquid crystal host W1825K.

the effective magnetic permeability of the nanoparticle has a resonant profile with positive and even negative values. In particular, considering the simulation for the ordinary refractive index of the LC, it presents a maximum positive value of 3.758 at 621 nm and a minimum negative value of −0.973 at 578 nm. Another interesting feature of these results is the fact that the magnetic response of the semiconductor nanoparticle can be tuned by changing the orientation of LC molecules. For the two possible extreme positions of LC molecules, an incident radiation "sees" the ordinary or the extraordinary refractive index of the LC, respectively. This magnetic anisotropy of the NP embedded in a LC can be clearly observed in Figure 2, where the effective magnetic permeability of the NP noticeably changes from the ordinary to the extraordinary case. As it can be seen, the maximum magnetic anisotropy occurs in the wavelengths around the maximum absolute values of the permeability.

The effective magnetic permeability of different nanoparticles embedded in a LC and the induced magnetic anisotropy have been calculated. The most remarkable results have been obtained considering liquid crystals W1825K and MLC6608.

Table 2: Maximum values of the effective magnetic permeability and magnetic anisotropy of an isolated nanoparticle made of different semiconductor materials (embedded in a W1825K LC host) for the ordinary and extraordinary cases. Radius of each NP that maximizes the permeability is also included.

NP mixture	μ_{ordinary}	$\mu_{\text{extraordinary}}$	$\Delta\mu_{\text{max}}$	R_{max}
AlAs	2.451	1.618	0.833	52
AlSb	3.758	2.297	1.487	58
GaAs	2.482	1.920	0.5828	85
GaInP	2.881	1.958	0.930	78
GaP	2.714	1.760	0.956	53
InGaAs	1.879	1.603	0.284	76
Si	3.001	2.105	0.931	70
TiO_2	2.001	1.439	0.570	79

Table 3: Minimum values of the nanoparticle permeability and magnetic anisotropy of semiconductor nanoparticles (embedded in a W1825K LC host) for the ordinary and extraordinary cases. Radius of each NP that minimizes the permeability is also included.

NP mixture	μ_{ordinary}	$\mu_{\text{extraordinary}}$	$\Delta\mu_{\text{max}}$	R_{max}
AlAs	0.246	0. 816	0.894	61
AlSb	−0.973	0.423	1.814	64
GaAs	−0.046	0.593	0.783	97
GaInP	−0.107	0.785	1.119	88
GaP	−0.087	0.755	1.117	58
InGaAs	0.250	0.656	0.456	90
Si	−0.423	0.474	1.193	78
TiO_2	0.585	0.991	0.532	94

Table 2 shows the results for W1825K. For each NP material, the permeability and magnetic anisotropy shown in the table have been calculated with a nanoparticle size that maximizes the permeability. This value is also included in Table 2. The profile of the permeability function at both ordinary and extraordinary cases allows the appearance of a nonunitary magnetic anisotropy in a range of incident wavelengths (see Figure 2). In addition, the magnetic anisotropy remains high in certain wavelengths range. This is a key fact for practical use of the proposed system.

Results shown in Table 2 consider maximum positive values of μ_s. Figure 2 also shows that there is magnetic anisotropy considering the smallest values of the magnetic permeability of the nanoparticles with the same LC host. Table 3 shows the minimum effective magnetic permeability and the anisotropy that have been observed. As in Table 2, these values have been calculated with nanoparticle sizes that minimize the permeability. As it can be seen, in some cases, negative values of μ_s can be achieved.

As it can be seen in previous results, the nanoparticle size is one of the key parameters in the appearance of magnetic resonances. Thus, the dependence of the effective permeability with the NP size has been analyzed in order to find the NP radius that maximizes μ_s value, as it has been observed in previous results. Figure 3 shows the effective permeability (μ_s) of the semiconductor NPs under study embedded in different LCs as a function of the NP size. Again, although every combination of NP material/LC host listed above has been considered, only the most noticeable results have been summarized. The radius range has been selected between 35 and 150 nm in order to ensure the appearance of the magnetic resonance in the visible range and to accomplish the dipole-like criterion. Both the ordinary (Figure 3(a)) and the extraordinary (Figure 3(b)) refractive indices of the LC have been considered. In both cases, the same behavior can be observed. As it was expected, there is an increase of μ_s as the NP radius increases, until it reaches a maximum value. Then, it slowly decreases until a certain NP size at which the value of μ_s drops to a value of 1 (no magnetic response). This behavior is related to the evolution of the magnetic resonance of the nanoparticle. When it arises, its height increases as the NP size increases until a maximum value. Then, although the NP size increases, the magnetic resonance broadens producing a decrease of the height until it disappears.

By comparing both figures (Figures 3(a) and 3(b)), it can be seen that there are important changes in the values, but not in the profile of the permeability, for a given NP-LC combination. The cases of Si and GaInP nanoparticles have shown a remarkable difference at the maximum values of permeability; thus, they have a high magnetic anisotropy for a large range of values of the particle size (R).

As it is also shown in Figure 3, the highest value of μ_s is achieved for an AlSb NP embedded in the liquid crystal MLC6608, with a value of 3.779, while that considering a W1825K LC is 3.758, both in the ordinary case. As it can be seen, the results using both LCs are quite similar. Other interesting NP materials having a pronounced peak of μ_s are GaP and GaInP.

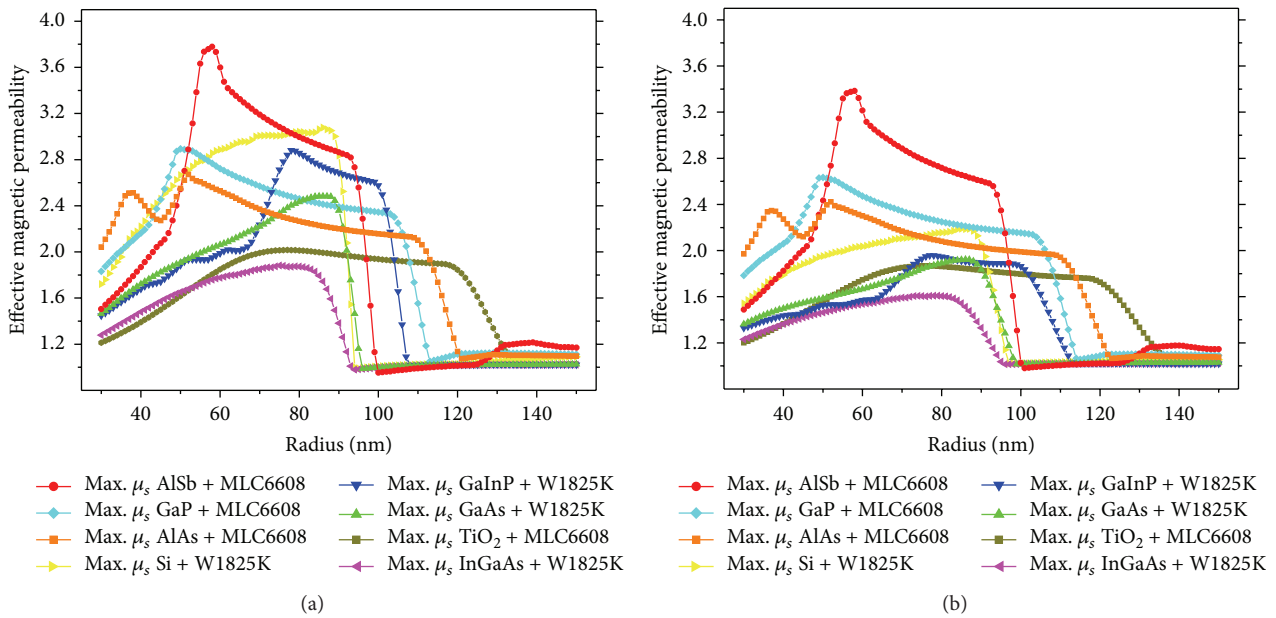

FIGURE 3: Evolution of the effective magnetic permeability (μ_s) of NPs embedded in a liquid crystal host as a function of the NP size when the refractive index of the host is either the ordinary component (a) or the extraordinary one (b).

3.3. Effective Permeability of Mixtures. The use of inclusions in a LC host is a well-known technique either to change the properties of the liquid crystal [38] or to actively control the optical properties of the NPs [17] In addition, as it was previously mentioned, the magnetism in liquid crystals is not a noticeable feature. However, in the previous section, it is showed that isolated semiconductor nanoparticles embedded in a liquid crystal host can present magnetic properties. In this sense, this section is devoted to analyze the effective magnetic permeability (μ_{eff}) of a sample composed of a LC doped with a certain concentration of these NPs. While the effective magnetic permeability (μ_s) of an isolated NP has been calculated previously, the permeability of the LC (μ_h) is equal to 1 in terms of relative permeability. To perform these calculations, the Maxwell-Garnett theory of effective index, previously explained, has been used. In order to maximize the global magnetic response, μ_{eff} has been calculated as a function of both the size of the doping nanoparticle and its concentration in the volume of the mixture (f). In addition, μ_{eff} has been calculated considering both the ordinary and extraordinary refractive indices of the LC, in order to observe if a magnetic anisotropy is also possible in the mixture.

The optimization of μ_{eff} regarding the two considered parameters, NP size and f, shows that the nanoparticles radius that maximize μ_{eff} is very similar to that producing maximum values of μ_s, with a slight variation in a range of 10 nm. This may occur as a result of the broadness in wavelength of μ_s function at the peak, as it is observed in Figure 2.

Figure 4 shows the spectral profile of the function μ_{eff} for the mixture W1825K LC doped with AlSb nanoparticles and for both components, ordinary and extraordinary. The radius of the nanoparticles and the volume fraction are 63 nm and 5%, respectively. As it was expected, this profile

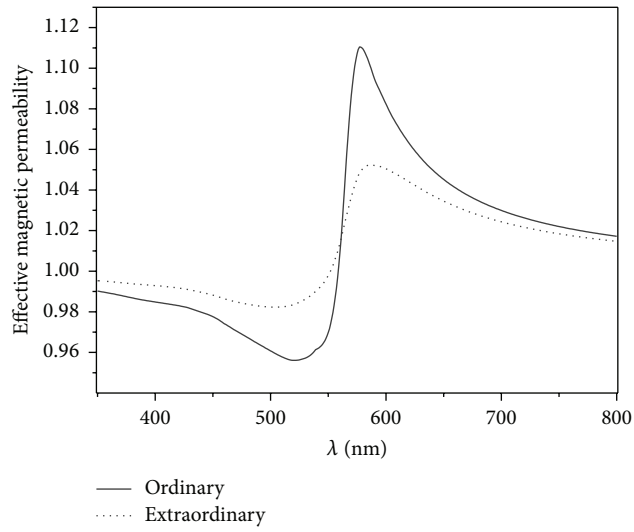

FIGURE 4: Effective magnetic permeability (μ_{eff}) of a composite of W1825K LC doped with AlSb (R = 63 nm) NPs with a volume fraction of 5% as a function of the incident wavelength. Both the ordinary and the extraordinary components of the LC properties have been considered.

is quite similar to that of the magnetic permeability of a single NP. However, the low concentration of NPs results in the fact that the magnitude of μ_{eff} is smaller than that of an isolated nanoparticle. In addition, the spectral stability of the magnetic resonance of these nanoparticles produces small values of the magnetic anisotropy. However, an effective magnetic anisotropy ($\Delta\mu$) can be clearly observed in the mixture.

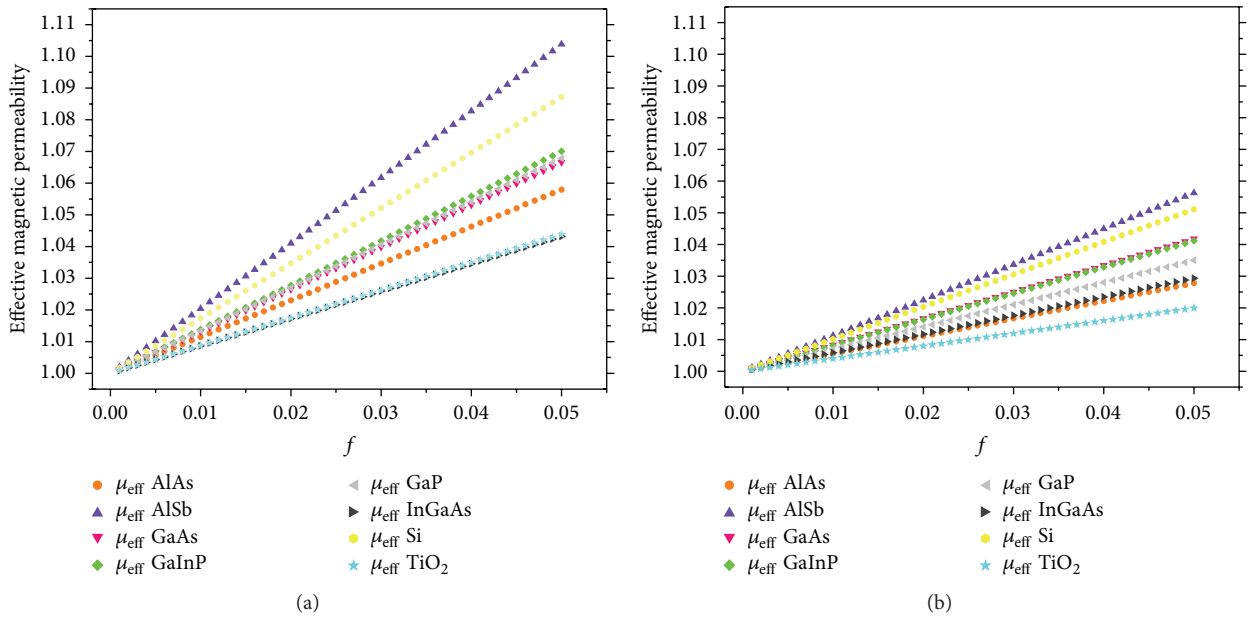

FIGURE 5: Evolution of μ_{eff} as a function of the volume fraction for each mixture considering (a) the ordinary component or (b) the extraordinary component of W1825K LC.

On the other hand, the concentration of the nanoparticles is also an important factor to manipulate the value of the effective permeability of the mixture. Simulations of the mixture with a fixed NP radius and changing f from 0.1% to 5% have been made. The fabrication of homogeneous NP-LC composites is not trivial in any case, but it is very complex if the NPs concentration is larger than 5% [39]. In experimental mixtures with high NP concentration, there is a high probability of nanoparticles aggregation that would distort measures of the permeability. Large values of f may also disturb the formation of the LC phase. Figure 5 shows the global effective magnetic permeability of the mixture as a function of the volume fraction, for the ordinary (Figure 5(a)) and extraordinary (Figure 5(b)) cases. The dopants are NPs of semiconductor materials whose size produces a maximum value of μ_s. As it can be seen, the value of f producing a maximum value of μ_{eff} is the maximum considered value of f. This result is expected from (1). Thus, the fabrication of samples with a high concentration of NPs is needed to obtain larger magnetic behaviors in this kind of mixtures. Despite the low values, by comparing both figures, a detectable magnetic anisotropy is observed. Thus, we can conclude that these composites would behave as magnetic anisotropic metamaterials.

4. Conclusions

While the dielectric anisotropy of liquid crystals is quite interesting for a large number of applications in several fields, these media do not have a remarkable magnetic response. On the other hand, interesting magnetic resonances arise in the light scattering of high-refractive-index semiconductor nanoparticles in the visible spectrum. In this work, the magnetic properties of mixtures combining both media (LC doped with semiconductor nanoparticles) have been theoretically studied.

Light scattering resonances of semiconductor nanospheres can be analyzed through the use of the Mie theory. By analyzing the first four Mie coefficients, it was observed that, around the magnetic resonances of these nanoparticles, there is a clear predominance of the dipolar terms over the quadrupolar ones. This means that these nanoparticles behave as dipole-like spheres, despite their real size. Thus, Mie coefficients can be drastically simplified.

Considering an isolated nanoparticle embedded in a LC, the effective permeability of the nanoparticle, under the Rayleigh assumption, has been deduced. In this case, a noticeable value of μ has been found, showing that the presence of the LC does not frustrate the appearance of these resonances. In addition, μ values change if ordinary or extraordinary refractive indices of the liquid crystal are used. Then, there is an externally induced magnetic anisotropy in the NP. Several semiconductor materials and LCs have been considered to maximize magnetic response. In addition, optimum sizes of the nanoparticles have been calculated.

On the other hand, if the mixture composed of a liquid crystal doped with these resonant nanoparticles in a certain volume fraction is considered, a new effective magnetic permeability of the mixture can be calculated using the Maxwell-Garnett effective medium theory. Thus, the mixture is considered as an effective medium or a metamaterial. All analyzed cases present a nonunitary permeability showing an effective magnetism in the mixture. However, these values of μ are much smaller than those calculated for the isolated particles. This fact is due to the contrast between the refractive index of the liquid crystal and that of the nanoparticle,

besides the low concentration of NPs in the mixture. Unfortunately, high concentrations of nanoparticles in a liquid crystal host cannot produce a stable and homogenous sample. High volume fraction of nanoparticles or devices with large surfaces compared with NPs size can improve these results. Despite the small values of the global effective permeability, an appreciable magnetic anisotropy can be calculated in these samples. Thus, a magnetic anisotropic media can be performed by means of these composites. This fact provides a new approach in the field of active magnetic devices and can be useful for the improvement or even new designs of them. For instance, a new sensor could be tested and used in significant potential applications like linear displacement and current sensing, gyroscope devices, or magnetic field detectors for technical/industrial purposes. Therefore, in future experimental works, a small sampling of these sensor capabilities will be presented.

Competing Interests

The authors declare that there is no conflict of interests regarding the publication of this paper.

Acknowledgments

This work has been supported by Ministerio de Economía y Competitividad of Spain (Grants nos. TEC2013-47342-C2-2-R, TEC2012-38901-C02-01, and TEC2013-50138-EXP) and the R&D Program SINFOTON S2013/MIT-2790 of the Comunidad de Madrid. Vicente Marzal acknowledges the Ministerio de Economía y Competitividad for FPI grant.

References

[1] M. L. Brongersma and P. G. Kik, Eds., *Surface Plasmon Nanophotonics*, Springer, Dordrecht, The Netherlands, 2007.

[2] F. J. Garcia-Vidal, L. Martín-Moreno, and J. B. Pendry, "Surfaces with holes in them: new plasmonic metamaterials," *Journal of Optics A: Pure and Applied Optics*, vol. 7, no. 2, pp. S97–S101, 2005.

[3] W. Cai and V. Shalaev, *Optical Metamaterials*, Springer, New York, NY, USA, 2010.

[4] B. García-Cámara, J. F. Algorri, A. Cuadrado et al., "All-optical nanometric switch based on the directional scattering of semiconductor nanoparticles," *The Journal of Physical Chemistry C*, vol. 119, no. 33, pp. 19558–19564, 2015.

[5] L. De Sio, G. Klein, S. Serak et al., "All-optical control of localized plasmonic resonance realized by photoalignment of liquid crystals," *The Journal of Materials Chemistry C*, vol. 1, no. 45, pp. 7483–7487, 2013.

[6] A. Alù and N. Engheta, "Emission enhancement in a plasmonic waveguide at cut-off," *Materials*, vol. 4, no. 1, pp. 141–152, 2011.

[7] S. I. Bozhevolnyi, *Plasmonic Nanoguides and Circuits*, Pan Stanford Publishing Pte, Singapore, 2009.

[8] V. N. Smolyaninova, I. I. Smolyaninova, A. V. Kildishev, and V. M. Shalaev, "Broadband transformation optics devices," *Materials*, vol. 3, no. 10, pp. 4793–4810, 2010.

[9] V. M. Shalaev, Ed., *Nanophotonics with Surface Plasmons*, Elsevier, Amsterdam, The Netherlands, 1st edition, 2007.

[10] A. García-Etxarri, R. Gómez-Medina, L. S. Froufe-Pérez et al., "Strong magnetic response of submicron Silicon particles in the infrared," *Optics Express*, vol. 19, no. 6, pp. 4815–4826, 2011.

[11] R. Gómez-Medina, B. García-Cámara, I. Suárez-Lacalle et al., "Electric and magnetic dipolar response of germanium nanospheres: interference effects, scattering anisotropy, and optical forces," *Journal of Nanophotonics*, vol. 5, no. 1, Article ID 053512, 2011.

[12] K. Vynck, D. Felbacq, E. Centeno, A. I. Căbuz, D. Cassagne, and B. Guizal, "All-dielectric rod-type metamaterials at optical frequencies," *Physical Review Letters*, vol. 102, no. 13, Article ID 133901, 2009.

[13] M. Kerker, D.-S. Wang, and C. L. Giles, "Electromagnetic scattering by magnetic spheres," *Journal of the Optical Society of America*, vol. 73, no. 6, pp. 765–767, 1983.

[14] J. M. Geffrin, B. García-Cámara, R. Gómez-Medina et al., "Magnetic and electric coherence in forward- and back-scattered electromagnetic waves by a single dielectric subwavelength sphere," *Nature Communications*, vol. 3, article 1171, 2012.

[15] C. M. Soukoulis, T. Koschny, J. Zhou, M. Kafesaki, and E. N. Economou, "Magnetic response of split ring resonators at terahertz frequencies," *Physica Status Solidi B*, vol. 244, no. 4, pp. 1181–1187, 2007.

[16] J. N. Anker, W. P. Hall, O. Lyandres, N. C. Shah, J. Zhao, and R. P. Van Duyne, "Biosensing with plasmonic nanosensors," *Nature Materials*, vol. 7, no. 6, pp. 442–453, 2008.

[17] Y. Zhang, Q. Liu, H. Mundoor, Y. Yuan, and I. I. Smalyukh, "Metal nanoparticle dispersion, alignment, and assembly in nematic liquid crystals for applications in switchable plasmonic color filters and E-polarizers," *ACS Nano*, vol. 9, no. 3, pp. 3097–3108, 2015.

[18] D. C. Zografopoulos, R. Beccherelli, A. C. Tasolamprou, and E. E. Kriezis, "Liquid-crystal tunable waveguides for integrated plasmonic components," *Photonics and Nanostructures—Fundamentals and Applications*, vol. 11, no. 1, pp. 73–84, 2013.

[19] W. Dickson, G. A. Wurtz, P. R. Evans, R. J. Pollard, and A. V. Zayats, "Electronically controlled surface plasmon dispersion and optical transmission through metallic hole arrays using liquid crystal," *Nano Letters*, vol. 8, no. 1, pp. 281–286, 2008.

[20] L. De Sio, G. Klein, S. Serak et al., "All-optical control of localized plasmonic resonance realized by photoalignment of liquid crystals," *Journal of Materials Chemistry C*, vol. 1, no. 45, pp. 7483–7487, 2013.

[21] L. De Sio, T. Placido, S. Serak et al., "Nano-localized heating source for photonics and plasmonics," *Advanced Optical Materials*, vol. 1, no. 12, pp. 899–904, 2013.

[22] I. Abdulhalim, "Liquid crystal active nanophotonics and plasmonics: from science to devices," *Journal of Nanophotonics*, vol. 6, no. 1, Article ID 061001, 2012.

[23] Y. J. Liu, G. Y. Si, E. S. P. Leong, N. Xiang, A. J. Danner, and J. H. Teng, "Light-driven plasmonic color filters by overlaying photoresponsive liquid crystals on gold annular aperture arrays," *Advanced Materials*, vol. 24, no. 23, pp. OP131–OP135, 2012.

[24] J. S. T. Smalley, Y. Zhao, A. A. Nawaz et al., "High contrast modulation of plasmonic signals using nanoscale dual-frequency liquid crystals," *Optics Express*, vol. 19, no. 16, pp. 15265–15274, 2011.

[25] R. Ruppin, "Evaluation of extended Maxwell-Garnett theories," *Optics Communications*, vol. 182, no. 4, pp. 273–279, 2000.

[26] C. F. Bohren and D. R. Huffman, *Absorption and Scattering of Light by Small Particles*, John Wiley & Sons, New York, NY, USA, 1983.

[27] C.-H. Wen, S. Gauza, J. Li, H. Wang, and S.-T. Wu, "High contrast homeotropic alignment of difluorotolane liquid crystals," *Liquid Crystals*, vol. 32, no. 5, pp. 643–649, 2005.

[28] E. Miszczyk, Z. Raszewski, J. Kdzierski et al., "Interference method for determining dispersion of refractive indices of liquid crystals," *Molecular Crystals and Liquid Crystals*, vol. 544, pp. 22–36, 2011.

[29] J. Li and S.-T. Wu, "Self-consistency of Vuks equations for liquid-crystal refractive indices," *Journal of Applied Physics*, vol. 96, no. 11, pp. 6253–6258, 2004.

[30] S. Kang, S. Nakajima, Y. Arakawa, G.-I. Konishi, and J. Watanabe, "Large extraordinary refractive index in highly birefringent nematic liquid crystals of dinaphthyldiacetylene-based materials," *Journal of Materials Chemistry C*, vol. 1, no. 27, pp. 4222–4226, 2013.

[31] J. Li, G. Baird, Y.-H. Lin, H. Ren, and S.-T. Wu, "Refractive-index matching between liquid crystals and photopolymers," *Journal of the Society for Information Display*, vol. 13, no. 12, pp. 1017–1026, 2005.

[32] J. Li, C.-H. Wen, S. Gauza, R. Lu, and S.-T. Wu, "Refractive indices of liquid crystals for display applications," *Journal of Display Technology*, vol. 1, no. 1, pp. 51–61, 2005.

[33] E. D. Palik and G. Ghosh, Eds., *Handbook of Optical Constants of Solids*, Academic Press, San Diego, Calif, USA, 1998.

[34] S. Zollner, C. Lin, E. Schönherr, A. Böhringer, and M. Cardona, "The dielectric function of AlSb from 1.4 to 5.8 eV determined by spectroscopic ellipsometry," *Journal of Applied Physics*, vol. 66, no. 1, pp. 383–387, 1989.

[35] G. E. Jellison Jr., "Optical functions of GaAs, GaP, and Ge determined by two-channel polarization modulation ellipsometry," *Optical Materials*, vol. 1, no. 3, pp. 151–160, 1992.

[36] M. Schubert, V. Gottschalch, C. M. Herzinger, H. Yao, P. G. Snyder, and J. A. Woolam, "Optical constants of Ga x in 1–x P lattice matched to GaAs," *Journal of Applied Physics*, vol. 77, no. 7, pp. 3416–3419, 1995.

[37] G. E. Jellison Jr., "Optical functions of silicon determined by two-channel polarization modulation ellipsometry," *Optical Materials*, vol. 1, no. 1, pp. 41–47, 1992.

[38] M. Urbanski and J. P. F. Lagerwall, "Nanoparticles dispersed in liquid crystals: impact on conductivity, low-frequency relaxation and electro-optical performance," *Journal of Materials Chemistry C*, vol. 4, no. 16, pp. 3485–3491, 2016.

[39] X. Li, C. Yang, Q. Wang et al., "Enhanced birefringence for metallic nanoparticle doped liquid crystals," *Optics Communications*, vol. 286, no. 1, pp. 224–227, 2013.